BJP British Journal of Pharmacology

DOI:10.1111/bph.13102
www.brjpharmacol.org

Themed Section: Epigenetics and Therapy

RESEARCH PAPER

# Pharmacological methyl group donors block skeletal metastasis *in vitro* and *in vivo*

Nicholas Shukeir[1,*,†], Barbara Stefanska[2,3,†], Surabhi Parashar[1], Flora Chik[2], Ani Arakelian[1], Moshe Szyf[2] and Shafaat A Rabbani[1]

[1]*Department of Medicine, McGill University Health Center, Montreal, QC, Canada,* [2]*Department of Pharmacology and Therapeutics, McGill University Health Center, Montreal, QC, Canada, and* [3]*Department of Nutrition Science, Purdue University, West Lafayette, IN, USA*

**Correspondence**
Dr Shafaat A Rabbani, McGill University Health Centre, 687 Pine Avenue West, Room H4.67, Montreal, QC, Canada H3A 1A1.
E-mail: shafaat.rabbani@mcgill.ca

*Present address: Max Planck Institute of Immunobiology and Epigenetics, Freiburg, Germany.

[†]The first two authors had an equal contribution.

**Received**
7 June 2014
**Revised**
19 January 2015
**Accepted**
22 January 2015

## BACKGROUND AND PURPOSE

DNA hypomethylation was previously implicated in metastasis. In the present study, we examined whether methyl supplementation with the universal methyl donor S-adenosylmethionine (SAM) inhibits prostate cancer associated skeletal metastasis.

## EXPERIMENTAL APPROACH

Highly invasive human prostate cancer cells PC-3 and DU-145 were treated with vehicle alone, S-adenosylhomocysteine (SAH) or SAM and their effects on tumour cell proliferation, invasion, migration and colony formation were monitored. For *in vivo* studies, control (SAH) and SAM-treated PC-3 cells were injected into the tibia of Fox chase SCID mice and skeletal lesions were determined by X-ray and μCT. To understand possible mechanisms involved, we delineated the effect of SAM on the genome-wide methylation profile of PC-3 cells.

## KEY RESULTS

Treatment with SAM resulted in a dose-dependent inhibition of tumour cell proliferation, invasion, cell migration, colony formation and cell cycle characteristics. Animals injected with 250 μM SAM-treated cells developed significantly smaller skeletal lesions, which were associated with increases in bone volume to tumour volume ratio and connectivity density as well as decreased trabecular spacing. Genome-wide methylation analysis showed differential methylation in several key signalling pathways implicated in prostate cancer including the signal transducer and activator of transcription 3 (*STAT3*) pathway. A selective STAT3 inhibitor decreased tumour cell invasion, effects which were less pronounced as compared with SAM.

## CONCLUSIONS AND IMPLICATIONS

These studies provide a possible mechanism for the role of DNA demethylation in the development of skeletal metastasis and a rationale for the use of hypermethylation pharmacological agents to impede the development and progression of skeletal metastasis.

## LINKED ARTICLES

This article is part of a themed section on Epigenetics and Therapy. To view the other articles in this section visit http://dx.doi.org/10.1111/bph.2015.172.issue-11

## Abbreviations

BV, bone volume; DNMT, DNA methyltransferase; GNMT, glycine N-methyltransferase; SAH, S-adenosylhomocysteine; SAM, S-adenosylmethionine; SCID, severe combined immune-deficient; STAT3, signal transducer and activator of transcription 3; TGFBR2, TGF-β receptor type II; TSS, transcription start site; TV, tumour volume; uPA, urokinase-type plasminogen activator

## Tables of Links

| TARGETS | |
|---|---|
| **GPCRs**[a] | **Enzymes**[d] |
| CXCR4 | ERK5 |
| **Nuclear hormone receptors**[b] | ILK |
| Glucocorticoid receptor | JAK1 |
| PPARα | JAK2 |
| RXRα | JAK3 |
| **Catalytic receptors**[c] | MMP2 |
| Ephrin B receptor | mTOR |
| ErbB2 (HER2) | PLC |
| ErbB3 | TYK2 |
| TGFBR2 | uPA |

| LIGANDS | |
|---|---|
| β-catenin | IL-15 |
| EGF | Oestrogen |
| Ethanol | Oncostatin |
| GNRH | PDGF |
| HGF | Prolactin |
| IGF-1 | S-adenosylhomocysteine (SAH) |
| IL-2 | S-adenosylmethionine (SAM) |
| IL-3 | TGF-β |
| IL-6 | VEGF |
| IL-9 | |

These Tables list key protein targets and ligands in this article which are hyperlinked to corresponding entries in http://www.guidetopharmacology.org, the common portal for data from the IUPHAR/BPS Guide to PHARMACOLOGY (Pawson *et al.*, 2014) and are permanently archived in the Concise Guide to PHARMACOLOGY 2013/14 ([a,b,c,d]Alexander *et al.*, 2013a,b,c,d).

## Introduction

Although slow growing, prostate cancer remains one of the most common lethal diseases in the Western world (Siegel *et al.*, 2013). Due to advances in screening and treatment of localized prostate tumours, mortality rates have steadied with even slight decreases being reported (Siegel *et al.*, 2013). However, development of distant metastases, particularly to the skeleton, still presents a major problem in curing the disease (Sturge *et al.*, 2011). Bone metastases develop through a series of events initiating with the dislodging of tumour cells from the parental primary tumour and breaking through the basement membrane (Gupta and Massague, 2006). The ability of detached tumour cells to avoid apoptotic mechanisms and the innate immunity allows them to eventually intravasate into the vascular system, get attracted to and colonize the preferred target organ (Steeg, 2006). Several key growth factors and proteases such as VEGF, PDGF, MMPs and urokinase plasminogen activator (uPA) facilitate the development of distant metastases by promoting tumour cell proliferation and angiogenesis (Heath and Bicknell, 2009; Kwaan and McMahon, 2009; Kessenbrock *et al.*, 2010).

The skeletal microenvironment is composed of several cell types including bone-forming osteoblasts, bone-resorbing osteoclasts and several other cell types (Bussard *et al.*, 2008). Chemokines secreted by the bone microenvironment attract circulating tumour cells through their actions on cell-surface receptors present on the tumour cells. Colonization of bone by tumour cells results in a vicious self-sustaining cycle whereby factors secreted by tumour cells deregulate proper osteoblast and/or osteoclast proliferation and maturation leading to factors being released by the bone matrix, which are tumour proliferative (Sun *et al.*, 2010; Suva *et al.*, 2011). Several factors have been implicated in the establishment and maintenance of the above-mentioned cycle and they include the TGF-β/bone morphogenetic proteins axis, the receptor activator of NF-κB ligand axis and the WNT signalling pathway (Chen *et al.*, 2004; 2006; Juarez and Guise, 2011; Jiang *et al.*, 2013). Moreover, a number of signalling pathways have been implicated in the development and progression of prostate cancer and noteworthy among those is the pathway involving the transcription factor signal transducer and activator of transcription 3 (STAT3), which has significant effects on cell survival, angiogenesis and gene expression regulation (Devarajan and Huang, 2009; Gu *et al.*, 2010). The eventual imbalance between osteoblasts and osteoclasts results in either bone forming (osteoblastic), bone resorbing (osteoclastic) or mixed lesions.

Although the focus of DNA methylation in cancer research has been on hypermethylation of tumour suppressor genes with consequent anti-cancer therapeutics focused on DNA methylation inhibitors, we have previously shown that hypomethylation might play a crucial role in cancer metastasis (Pakneshan *et al.*, 2004; Ateeq *et al.*, 2008). We have recently delineated the landscape of DNA demethylation in liver cancer and demonstrated that the hypomethylated and hypermethylated promoters are equivalent in number, and that the hypomethylated genes are particularly enriched in pathways involved in cell invasion and metastasis (Stefanska *et al.*, 2011). Treatment of cells with the DNA methylation inhibitor 5-aza-deoxycytidine increased invasiveness of breast cancer cells through demethylation of pro-metastatic genes, and inhibition of this demethylation by treating the cells with S-adenosylmethionine (SAM), the universal methyl donor for methylation reactions, hypermethylates and silences the pro-metastatic genes reversing the pro-invasive effect of 5-aza-deoxycytidine (Chik *et al.*, 2014). Previously, we have reported the ability of SAM to increase methylation of pro-metastatic genes that are hypomethylated in invasive cancer such as *uPA* and *MMP2* and reduce breast and prostate cancer invasiveness and tumourigenesis both *in vitro* and *in vivo* (Pakneshan *et al.*, 2004; Shukeir *et al.*, 2006). We therefore hypothesized that bone metastasis, one of the main causes of prostate cancer morbidity and mortality, might also be driven by hypomethylation of genes needed for invading bone and that treatment with SAM should block prostate

cancer bone metastasis. We tested this hypothesis by utilizing the highly metastatic human prostate cancer PC-3 cell line, which develops osteolytic bone lesions. Pharmacological concentrations of SAM have also been shown to be of therapeutic value in several other diseases (Anstee and Day, 2012; Lee *et al.*, 2012). Additionally, the results of our study are of particular interest since SAM is an approved nutritional supplement and intracellular SAM levels can be modulated through dietary intake. Therefore, we believe that our findings offer interesting opportunities for controlling bone metastasizing prostate cancer.

## Methods

### Cell culture

Early-stage, low-invasive LNCaP and late-stage, highly invasive PC-3 and DU-145 human prostate cancer cells were obtained from the American Type Culture Collection. Cells were maintained in RPMI 1640 with 10% FBS, 2 mmol·L$^{-1}$ L-glutamine and 100 U·mL$^{-1}$ penicillin/streptomycin sulfate. Cells were incubated with different doses of SAM or S-adenosylhomocysteine (SAH; New England Biolabs, Mississauga, Ontario, Canda) as previously described (Shukeir *et al.*, 2006). STAT3 inhibitor S3I-201 was purchased from Cedarlane, Burlington, Ontario, Canada.

### Cell proliferation, invasion, wounding and colony formation assay

PC-3 and DU-145 cells were plated at a density of $5 \times 10^4$ cells per well in 6-well plates in 2 mL of culture media. Initially, a wide range of SAM doses (50–500 μM) were tested for their efficacy in *in vitro* studies based on previously established effective concentrations (Shukeir *et al.*, 2006). The effective SAM doses for the current study were established to be 100 μM and 250 μM, which, respectively, exhibited moderate to strong inhibitory effects on cell growth and invasive properties in both PC-3 and DU-145 cells. The invasive capacity of PC-3 and DU-145 cells was examined using a two-compartment Boyden chamber invasion assay (Costar Transwell, Corning Corporation, Sigma-Aldrich, Oakville, Ontario, Canada) following treatment with SAH (used as control) or SAM for 6 days as described previously (Shukeir *et al.*, 2006). For wound-healing analysis, PC-3 and DU-145 cells were treated with SAH or SAM for 6 days in the presence of 10% FBS. Cells were then plated in 6-well plates to form a monolayer and then wounded manually with a sterile 1000 μL pipette tip in the center of each well. Cells were grown in the presence of 2% FBS and migrating cells were photographed at different time points. Analysis and quantification was carried out using the Image Pro-Plus software (Media Cybernetics, Inc, Rockville, MD, USA) and calculated as percentage wound healing using the equation: % wound healing = [1 – (wound area at Tx h/wound area at $T_0$)], where Tx is the respective time point and $T_0$ is the time immediately after wounding. Three independent experiments were performed ($n = 3$).

For colony formation assay, $3 \times 10^3$ PC-3 and DU-145 cells, previously treated with SAH (250 μM) or SAM (100 μM and 250 μM) for 6 days, were seeded in triplicate into 6-well Petri dishes in the presence of 4 mL of culture medium containing 1.5% agar solution at 37°C. Medium was changed every 48 h. After 14 days post-plating, the number of colonies containing more than 100 cells was recorded. In other studies, PC-3 cells were treated with different doses (10–50 μM) of the STAT3 inhibitor (S3I-201) and the effects on cell proliferation and invasion were examined.

### FACS analysis

PC-3 and DU-145 cells were treated with SAH (250 μM) or SAM (100 and 250 μM) every 48 h for 6 days and then fixed by adding 70% ice-cold ethanol. Fixed cells were washed with PBS and then treated with 1U of DNase-free RNase followed by staining with 0.05 mg of propidium iodide overnight. FACS analysis was performed on a Calibur machine. Results were analysed further using the FlowJo software (FlowJo LLC, Ashland, OR, USA).

### Quantitative real-time PCR (qPCR)

Total cellular RNA from vehicle and SAM-treated cells was extracted using TRIzol (Invitrogen Life Technologies, Burlington, Ontario, Canada) according to the manufacturer's protocol. Two micrograms of total RNA was used for reverse transcription; 2 μL of cDNA was then used in a 20 μL PCR reaction containing SYBR green mix and 0.5 μM of forward and reverse primers. PCR was then performed in an ABI StepOne Plus with the following conditions: denaturation at 95°C for 10 min, amplification for 45 cycles at 95°C for 10 s, annealing temperature for 10 s, 72°C for 10 s, and final extension at 72°C for 10 min. Real-time qPCR analysis was carried out using the comparative ΔΔCt method.

### Illumina methylation 450K analysis

Genomic DNA was quantified using Picogreen protocol (Quant-iT™ PicoGreen® dsDNA Products, Invitrogen, P-7589) and read on a SpectraMAX GeminiXS Spectrophotometer (Molecular Devices LLC, Sunnyvale, CA, USA). Bisulfite conversion of 500 ng of genomic DNA was performed using the EZ-96 DNA Methylation-GOLD Kit (Zymo Research, Irvine, CA, USA). The Illumina Methylation 450K kit (Illumina, Inc, San Diego, CA, USA) was used for the microarray experiment as described by the manufacturer's protocol, except that 8 μL of bisulfite converted template was utilized to initiate the amplification step. The Illumina Hybridization oven was used for incubating amplified DNA (37°C) and for BeadChips hybridization (48°C). A Hybex incubator (SciGene, Sunnyvale, CA, USA) was used for fragmentation (37°C) and denaturation (95°C) steps. The X-stain step was carried out in a Tecan Freedom evo robot with a Te-Flow module. Arrays were scanned in Illumina iScan Reader. Data analysis was performed with the Methylation module (version 1.9.0) of the GenomeStudio software (Illumina; version 2011.1) using HumanMethylation450_15017482_v1.2.bpm manifest. GenomeStudio uses combined algorithms of statistical power calculation to provide a sensitive determination of methylation detection and differential methylation. Statistical threshold was set at a false discovery rate of >0.05, differential score (statistical power) of >13 and Δ β (differential methylation) between the groups was set at >0.15.

### Animal protocols

For *in vivo* studies, PC-3 cells were treated with SAH (250 μM), as control, or SAM (250 μM) for 6 days in RPMI+10% FBS. At

the end of the treatment, cells were harvested in sterile saline. Twenty 6-week-old male Fox Chase severe combined immune-deficient (SCID) mice, obtained from Charles River, St. Constant, Quebec, Canada, were randomly divided into two groups with 10 animals in each group (SAH, SAM 250). This number of animals per group ($n = 10$) is based on results of previous experiments and power calculations for detecting a 15% change in tumour growth, $\alpha = 0.05$ and $\beta = 0.8$ (Stefanska *et al.*, 2014). Mice were anaesthetized using a cocktail of ketamine (50 mg·kg$^{-1}$), xylazine (5 mg·kg$^{-1}$) and acepromazine (1 mg·kg$^{-1}$) injected i.m.; $2 \times 10^5$ of both control (SAH) and experimental PC-3 cells (SAM 250 μM) suspended in 40 μL of saline were injected into the left tibia using a 27-gauge needle. The mice were monitored weekly for tumour burden. At week 4, a digital radiography of hindlimbs of all animals was carried out using a Faxitron X-ray machine (Faxitron X-ray Corp, Lincolnshire, IL, USA) to monitor the development of skeletal lesions. The mice were then killed and the left tibias collected and fixed in 10% buffered formalin solution for 24 h. The X-ray scoring method is described as follows: no lesions or minor changes, small lesions, significant lesions (minor peripheral margin breaks, 1–10% of bone surface disrupted), and highly significant lesions (major peripheral margin breaks, >10% of bone surface broken) rating 0 to 4 respectively. The whole tibia (trabecular and cortical) of four representative animals from each group was analysed by micro-computed tomography with a SkyScan 1072 scanner and associated analysis software (SkyScan, Bruker microCT, Kontich, Belgium). Image acquisition was done at 45 kV with a 0.9 rotation between frames. During scanning, the tibias were enclosed in a tightly fitted plastic wrap to prevent movement and dehydration. All experimental animal protocols were in accordance with the McGill University Animal Care Committee guidelines. All studies involving animals are reported in accordance with the ARRIVE guidelines for reporting experiments involving animals (Kilkenny *et al.*, 2010; McGrath *et al.*, 2010).

### *Statistical analysis*

Data were assessed by one-way ANOVA followed by Tukey's *post hoc* test. Data are given as the mean ± SD of three independent experiments. The results are considered as statistically significant when $P < 0.05$.

## Results

### *Effect of SAM on prostate cancer cell proliferation, invasion and migration*

DNA hypomethylation in cancer particularly targets and activates genes involved in metastasis, cell migration and cell invasion. Our previous studies suggested that SAM treatment could lead to silencing of certain pro-metastatic genes. We therefore examined the effect of SAM and its inactive analogue SAH as control on cancer growth properties and invasiveness of two highly invasive human prostate cancer cell lines PC-3 and DU-145. Treatment of both cell lines with 100 μM and 250 μM SAM resulted in a significant inhibition of cell proliferation as compared with control cells during the same time period. These effects were more pronounced in DU-145 cells where 100 μM SAM exhibited maximum inhibition on cell proliferation following 7 days of treatment (Figure 1A).

The invasive capacity of both PC-3 and DU-145 was determined by Boyden chamber Matrigel invasion assay. Treatment of both cell lines with SAM reduced tumour cell invasion in a dose-dependent manner (Figure 1B). Determination of the number of tumour cells in both the upper and lower part of the Boyden chamber showed similar number of tumour cells during this treatment period demonstrating that the observed anti-invasive effects are independent of the anti-proliferative effects of SAM as shown in Figure 1A.

We then examined the effect of SAM on cell migration by a wound-healing assay. In these studies, PC-3 and DU-145 cells were treated with SAH (250 μM) or with different concentrations of SAM (100 and 250 μM) followed by evaluation of cell migration capacity at various time points. SAM treatment of these tumour cells decreased their migratory ability at all times compared with SAH-treated control cells. 250 μM SAM was most effective in blocking cell migration, which was quite pronounced at 48 h as shown in representative photomicrographs (Figure 1C). No such effect on cell proliferation, invasion and migration was seen on both PC-3 and DU-145 cells following treatment with vehicle alone and SAH throughout these studies (data not shown).

### *Effect of SAM on prostate cancer cell colony formation and cell cycle*

The ability of tumour cells to form colonies in soft agar is an index of their aggressive potential. We therefore examined the effect of SAM on the number of colonies formed by PC-3 and DU-145 cells. Following treatment of these cells with 100 and 250 μM SAM, a significant and dose-dependent decrease in the number of colonies formed was observed compared with control (SAH-treated) group of cells (Figure 2A). In order to elucidate the anti-proliferative effects of SAM, we then examined the effect of different doses (100 and 250 μM) on cell viability and on cell cycle kinetics. While no significant effects were seen on PC-3 and DU-145 cell viability, FACS analysis of cell cycle distribution of control and SAM-treated cells showed a significant dose-dependent increase in the number of cells arrested in the $G_2$/M phase following SAM treatment (Figure 2B).

### *Effect of SAM on PC-3 cells experimental skeletal metastasis* in vivo

Prostate cancer is one of the most common malignancies associated with skeletal metastasis. This is attributed to the expression of pro-metastatic genes by tumour cells and the induction of bone related genes leading to the development of osteoblastic lesions that eventually turn into the osteolytic variety. We next examined the effect of SAM on the development and progression of skeletal metastasis in our xenograft model of prostate cancer using the highly metastatic PC-3 cells, which, when injected into mice tibia, almost always develop into osteolytic lesions that can be easily monitored for lesion progression. Control and experimental cells treated with 250 μM SAH or SAM, respectively, for 6 days were inoculated directly into the tibia of male SCID mice as described in 'Methods'. Control animals (injected with SAH-treated cells)

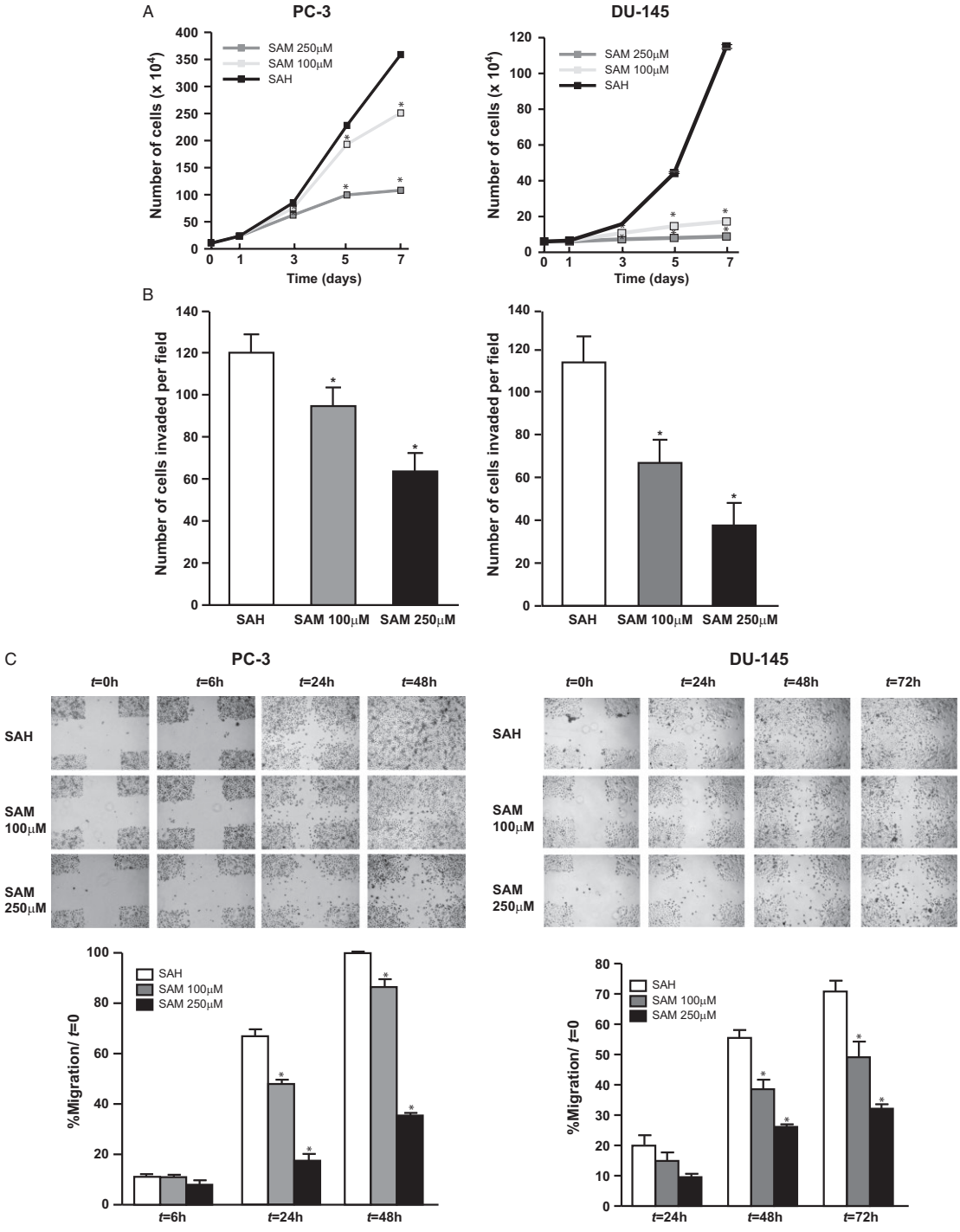


## Figure 1

Effect of SAM on prostate cancer cells proliferation, invasion and migration *in vitro*. Human prostate cancer cells PC-3 and DU-145 were plated in 6-well plates and treated with 250 μM of SAH as control (SAH) or two doses (100 and 250 μM) of SAM. Cell growth rate was determined in each group by trypsinization and counting the number of cells by Coulter counter as described in Methods (A). PC-3 and DU-145 cells' invasive capacity was evaluated by using a Boyden chamber Matrigel invasion assay. After 18 h of SAH (250 μM) or SAM (100 and 250 μM) treatment, the invaded cells were fixed, stained and 10 random fields were counted. Number of cells invading is shown as bar diagram ± SD (B) as described in Methods. Wound healing assay was carried out by seeding PC-3 and DU-145 cells in 6-well plates and allowing them to grow as a monolayer and making a wound as described in Methods. These cells were treated with either 250 μM SAH or two different doses of SAM (100 and 250 μM) containing 2% FBS and migrating cells were photographed at different time points (C). Wound healing was recorded at different time points, and % of wound healing with respect to $T_0$ was calculated using the equation described in Methods. Results are presented as the mean ± SD of three independent experiments ($n = 3$) from control and experimental cells. Significant differences from control (SAH) were determined using ANOVA followed by Tukey's *post hoc* test and are represented by an asterisk ($P < 0.05$).

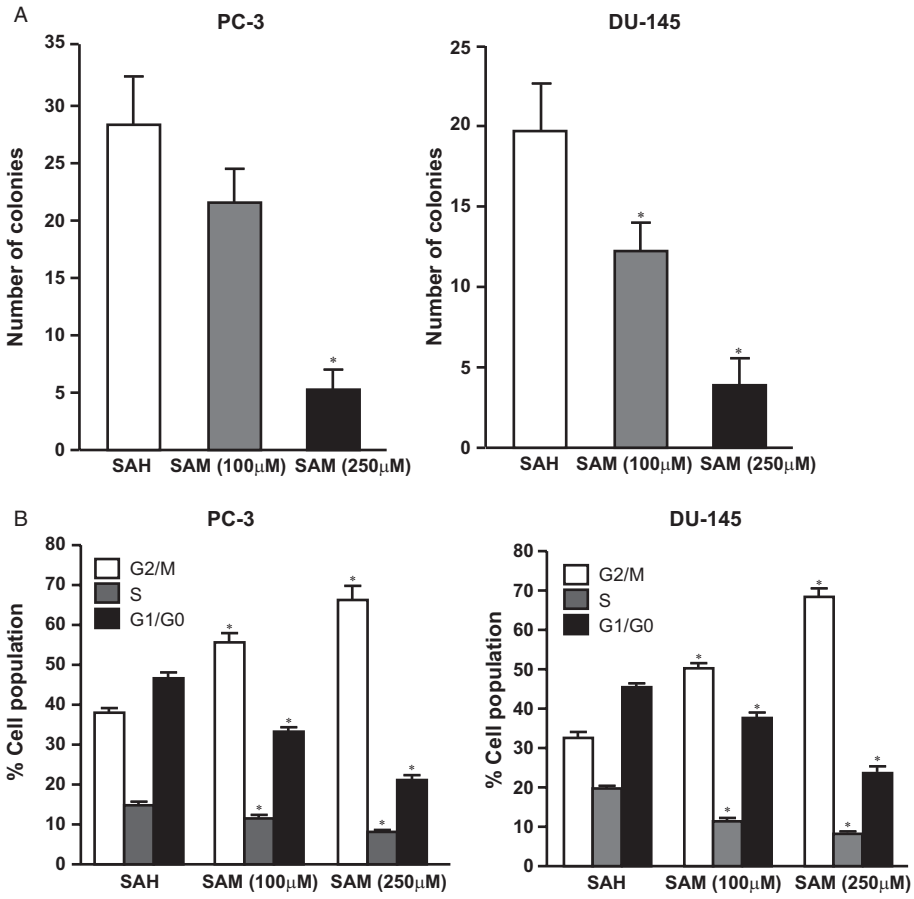


## Figure 2

Effect of SAM on colony formation and cell cycle kinetics of prostate cancer cells *in vitro*. PC-3 and DU-145 cells were plated onto soft agar for anchorage-independent growth in the presence of 250 μM SAH as control (SAH) or SAM (100 and 250 μM). Number of colonies was counted as described in Methods (A). PC-3 and DU-145 cells were treated with either SAH (250 μM) or SAM (100 and 250 μM). Treated cells were then fixed and stained with propidium iodide. FACS analysis was performed as described in Methods (B). Results are presented as the mean ± SD of three independent experiments ($n$ = 3) from control and experimental cells. Significant differences from control (SAH) were determined using ANOVA followed by Tukey's *post hoc* test and are represented by an asterisk ($P < 0.05$).

developed lesions at week 2, which continued to increase in size over time. In contrast, animals inoculated with PC-3 cells, pretreated with SAM exhibited reduced total skeletal lesions (~40%) compared with the control group at week 4 post-tumour cell inoculation (Figure 3). At the end of these studies, the tibia were removed and subjected to micro-computed tomography (μCT). Results from the μCT clearly demonstrated that SAM treatment leads to a marked reduction in skeletal lesions (Figure 4A). These effects of SAM led to increased bone volume to tumour volume (BV/TV) ratio, significantly decreased trabecular spacing and increased connectivity density in experimental animals (Figure 4B).

In all *in vivo* studies presented in Figures 3 and 4, no significant difference in animal weight was observed among control and experimental groups (data not shown). Collectively, analysis of skeletal lesions by these different methods (X-ray, μCT) consistently showed the ability of SAM to markedly reduce skeletal tumour burden.

### *Effect of SAM on prostate cancer associated gene expression*

In order to elucidate a possible molecular mechanism of these observed effects of SAM, we then examined the ability of SAM to alter the expression of various well-described genes known to play important roles in prostate cancer growth and skeletal metastasis. The data in Figure 5 show the results of qPCR analysis of mRNA expression from control (treated with 250 μM SAH) and experimental PC-3 cells treated with 250 μM SAM for 6 days, dose and time, which were found to be most effective at inhibiting tumour cell proliferation, invasion, migration, colony formation *in vitro* and reducing skeletal lesions *in vivo* as described above. We have previously demonstrated that SAM treatment led to increased methylation and silencing of *uPA* and *MMP2* in PC-3 cells (Shukeir *et al.*, 2006). We therefore confirmed the ability of SAM to reduce the expression of the pro-metastatic gene *uPA*. More significantly, we show additional pro-metastatic genes, which

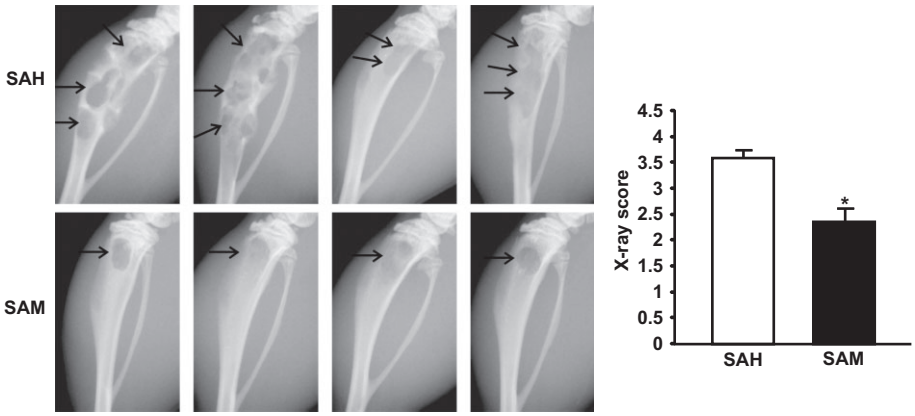


**Figure 3**

Effect of SAM on prostate cancer skeletal lesions *in vivo*. Male Fox Chase SCID mice were inoculated with $2 \times 10^5$ PC-3 cells treated with 250 μM SAH as control (CTL, $n = 10$) or 250 μM SAM ($n = 10$) for 6 days via intra-tibial route. Development of skeletal lesions was determined at weekly intervals by X-ray using Faxitron and lesion area was determined as described Methods. Four representative X-rays and lesion score of all control and experimental animals at week 4 post-tumour cell inoculation are shown. Skeletal lesions are indicated by arrows. The results in the graph represent the mean ± SEM of 10 animals in each group. Significant differences from control are represented by asterisks ($P < 0.05$).

are affected by SAM treatment; *TGF-β*, TGF-β receptor II (*TGFBR2*) and *RUNX2*, all of which play significant roles in the development and progression of skeletal metastases and bone remodelling (Figure 5A). Due to the methylating ability of SAM, we examined its effect on the expression of tumour suppressor genes like ras-associated domain family-1 isoform A and glutathione-s-transferase type P1. Real-time PCR analysis showed no significant change in the levels of expression of these genes following treatment of prostate cancer cells by SAM (Supporting Information Fig. S1).

## *Genome-wide analysis of the effects of SAM on DNA methylation states and the functional gene pathways affected*

One established mechanism of action of SAM is increasing DNA methylation through either increasing DNA methyltransferase (DNMT) activity or reducing demethylation activity (Detich *et al.*, 2003). As we have previously proposed, another potential mechanism for SAM action in invasive cancer cells would be by reversing the demethylation state of genes critical for invasion and metastasis. Several candidate genes were previously shown to be hypermethylated in response to SAM in invasive prostate and breast cancer cells (Pakneshan *et al.*, 2004; Shukeir *et al.*, 2006), but the genome-wide impact of SAM is unclear. As SAM is a general methyl donor, one concern might be that it could lead to widespread silencing and re-methylation of tumour suppressor genes. We therefore used a genome-wide approach to address this concern. The Illumina 450K array provides representative coverage of CpGs not only at transcription start sites (TSS) and 5′ regulatory regions, but also at gene bodies, CpG shores and 'open sea' with the latter referring to regions more than 4 kb from CpG islands. Surprisingly, in spite of the fact that SAM is a general methyl group donor, the DNA methylation changes were limited in scope and markedly specific. The Illumina methylation microarray of PC-3 and PC-3-SAM cells revealed that SAM treatment caused significant hypermethylation of 73 CpG sites [Δ β (differential methylation value: SAM–control) ≥ 0.15, differential score ≥ 13 equivalent to $P < 0.05$] corresponding to 51 genes involved in key intracellular signalling pathways that could affect tumour growth and metastasis (Table 1 and Supporting Information Table S1). Among the hypermethylated genes, we found strong oncogenes including CTSH and TTC23 associated with malignant prostate cancer and cervical cancer, respectively, transcriptional regulators including STATs, SRY, MIER2 and HSFY1, and regulators of signal transduction (e.g. STAT3, STAT5A, STAT5B, NXN). Functional analysis of genes hypermethylated upon SAM exposure using the ingenuity pathway analysis (IPA) revealed signalling pathways that mediate cell proliferation, migration, invasiveness, angiogenesis and metastasis, such as JAK/STAT, ERK/MAPK, WNT/β-catenin, mTOR, PPARG, VEGF, Gap and tight junction. Interestingly, SAM affects only a small fraction of the genes that are hypomethylated in invasive PC-3 cells relative to non-invasive LNCaP cells (Table 1). However, the vast majority of genes that are hypermethylated with SAM treatment (42 out of 51) were demethylated in invasive PC-3 cancer cells relative to non-invasive LNCaP cells suggesting that SAM reverses the demethylation of genes whose demethylation state is associated with the invasive phenotype. The Illumina data has been submitted to GEO under accession number GSE62053.

## *Role of STAT3 in SAM-mediated effects in prostate cancer*

One of the top canonical pathways identified by the IPA to be hypermethylated in response to SAM was the JAK/STAT pathway (Table 2), with hypermethylation of CpGs detected in the *STAT3*, *STAT5A* and *STAT5B* genes (Supporting Information Table S1). A CpG site located within a CpG island in the STAT3 promoter region showed the most extensive hypermethylation with Δ β value 0.23 (differential methylation between SAM and control) and differential score 98 ($P < 0.001$). Since STAT3 is involved in several pathways impli-

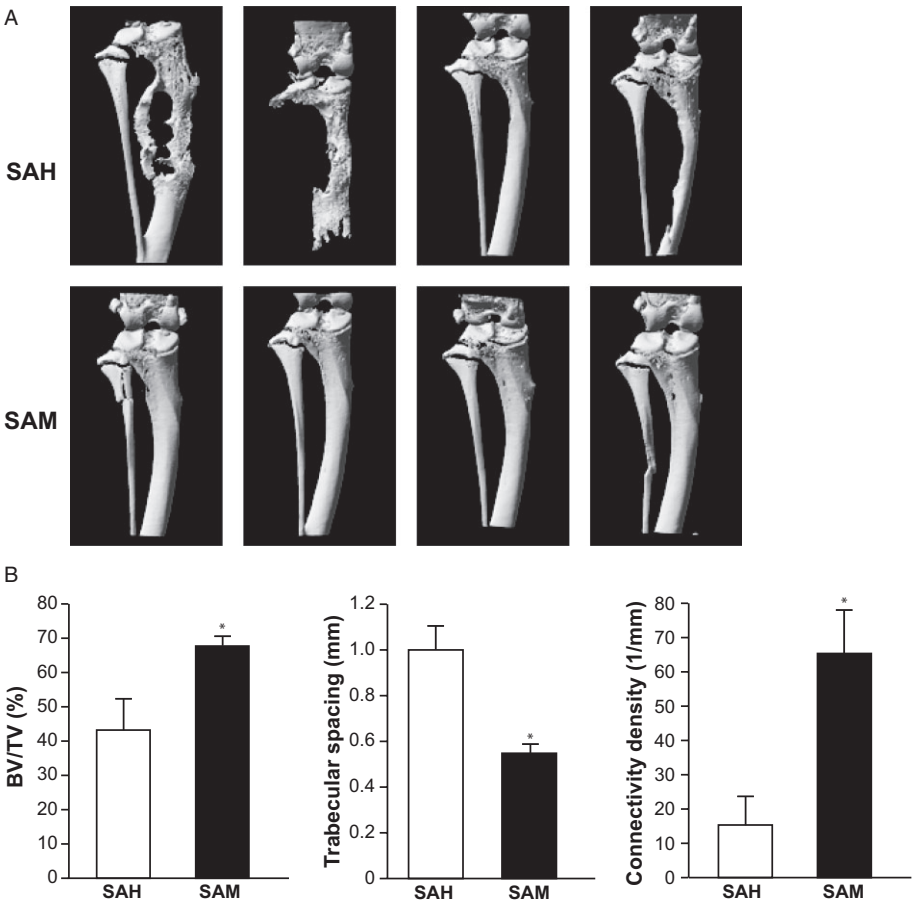


## Figure 4

Effect of SAM on prostate cancer skeletal lesion *in vivo* by micro-computed tomography (μCT). Male Fox Chase SCID mice were inoculated with $2 \times 10^5$ PC-3 cells treated with 250 μM SAH as control (CTL, $n = 10$) or 250 μM SAM ($n = 10$) for 6 days via i.t. route. At week 4 post-tumour cell inoculation, all animals were killed and their tibia collected and fixed. Tibias from four representative animals in each group underwent analysis by μCT with SkyScan and the frontal view is shown (A). The % BV/TV, trabecular spacing and connectivity density (B) was determined by the Skycan software as described in Methods. Significant differences from control are represented by asterisks ($P < 0.05$).

cated in invasion and metastasis, we first examined STAT3 expression in SAM-treated PC-3 cells. Real-time PCR analysis revealed that SAM caused a marked down-regulation of STAT3 expression and its downstream targets *BAX* and *Cyclin D* genes that are involved in apoptosis and cell cycle respectively (Figure 5B). In order to test the hypothesis that STAT3 plays a causal role in PC-3 invasiveness, and therefore its silencing by SAM treatment partly mediates the anti-invasive effects of SAM, we compared the effects of a selective STAT3 inhibitor (S3I-201) and SAM on PC-3 cells invasion. Both SAM and S3I-201 treatment led to reduced invasive capacity of treated PC-3 cells (Figure 5C). Interestingly, the anti-invasive effects were more pronounced following treatment with SAM as compared with S3I-201, which can be attributed to the broad ability of SAM to affect several additional signalling/oncogenic pathways implicated in tumour progression as shown in Table 2 (highlighted zones) compared with the selective activity of S3I-201 to target STAT3 only.

## Discussion

The first epigenetic change observed during the early stages of prostate cancer development is the hypermethylation at CpG islands of promoter regions of tumour suppressor genes (Fernandez *et al.*, 2012). It is now accepted that this early promoter hypermethylation leads to repression of several tumour suppressor genes such as *GSTP1*, *RASSF1A*, *APC* and *MDR1* among others (Mishra *et al.*, 2010; Richiardi *et al.*, 2013). The main focus in understanding the role of DNA methylation in cancer and subsequent strategies for treatment has been on inhibitors that cause DNA demethylation. However, it is becoming clear that, in cancer, promoter hypomethylation is as prevalent as hypermethylation (Stefanska *et al.*, 2011). For example, a recent mapping of the DNA methylation landscape in liver cancer revealed a similar number of hypomethylated and hypermethylated genes (Stefanska *et al.*, 2011). Interestingly, the hypomethylated genes are mainly known to be involved in cell invasion and

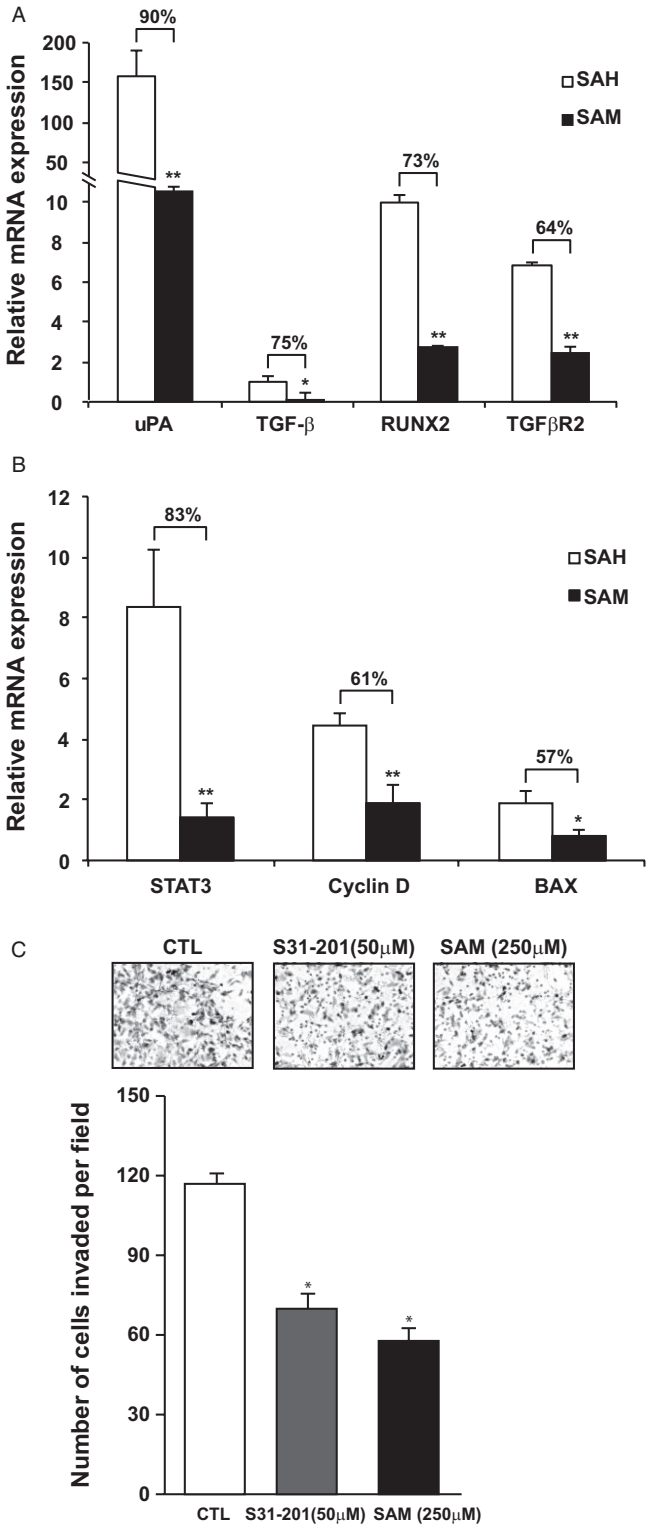


## Figure 5

Effect of SAM on the expression of genes associated with prostate cancer progression and skeletal metastasis, on STAT3 and downstream targets and the impact of selective STAT3 inhibitor (S3I-201) on PC-3 cell invasion. (A) PC-3 cells were treated with 250 μM SAH as control (SAH) or with 250 μM SAM for 6 days, and total cellular RNA was isolated with TRIzol. RNA from control and treatment groups was analysed for the expression of genes involved in tumour progression and skeletal metastasis. Changes in the mRNA expression of the representative genes were determined by plotting the relative ratio against *GAPDH*, which was used as a loading control. Results are presented as the mean ± SD of three independent experiments ($n = 3$) from control and experimental cells. Significant differences from control (SAH) are represented by asterisk(s) ($^*P < 0.05$, $^{**}P < 0.01$). (B) PC-3 cells were treated with 250 μM SAH as control (SAH) or with 250μ SAM for 6 days, and total cellular RNA was isolated with TRIzol. RNA from control and treatment groups was analysed for the expression of *STAT3*, *Bax* and *Cyclin D*. Changes in the mRNA expression of the representative genes were determined by plotting the relative ratio against *GAPDH*, which was used as loading control (A). Results are presented as the mean ± SD of three independent experiments ($n = 3$) from control and experimental cells. Significant differences from control (SAH) are represented by asterisk(s) ($^*P < 0.05$, $^{**}P < 0.01$). (C) PC-3 cells were treated with vehicle alone as control (PC-3), 250 μM SAM or 50 μM of STAT3 inhibitor S3I-201 and invasive capacity was evaluated by using a Boyden chamber Matrigel invasion assay. After 18h of SAM and S3I-201 treatment, the invaded cells were fixed, stained and 10 random fields were counted. Representative fields are depicted in the upper panel. Number of cells invading is shown as bar diagram ± SD (lower panel C) as described in Methods. Results are presented as the mean ± SD of three independent experiments ($n = 3$) from control and experimental cells. Significant differences from control (vehicle) were determined using ANOVA followed by Tukey's *post hoc* test and are represented by an asterisk ($P < 0.05$).

metastasis. Our Illumina 450K genome-wide analysis of differential methylation between non-invasive LNCaP and highly invasive PC-3 prostate cancer cell lines shows a large number of genes that are hypomethylated in PC-3 cells relative to LNCaP cells (Table 1). We have previously shown demethylation of several candidate genes in breast and prostate cancer to be critical for invasiveness and metastatic potential (Pakneshan *et al.*, 2004; Shukeir *et al.*, 2006; Ateeq *et al.*, 2008). This calls for a change in epigenetic cancer therapy strategies that also target the reversal of demethylation of critical metastasis genes by utilizing agents, which could lead to an increase in DNA methylation. While it is not fully elucidated why the overall levels of methylcytosine decrease during the progression of the disease, a possible explanation could be insufficient amounts of the methyl group donor SAM (Hoffmann and Schulz, 2005). Although SAM is not itself a methylating agent, it is a donor of the methyl group in the DNA methylation reaction catalysed by DNMTs. We have previously shown that SAM inhibits DNA demethylation activities as a potential mechanism that might result in altered DNA methylation states following SAM treatment (Detich *et al.*, 2003).

Disturbances in SAM/SAH ratio can lead to changes in the DNA methylation patterns and cell transformation. For instance, ethanol intake changes the metabolism of SAM leading to its depletion and decrease in SAM/SAH ratio, which subsequently results in global DNA hypomethylation,

## Table 1

Summary of DNA methylation differences between PC-3 cells treated with SAM (PC-3-SAM), control cells (PC-3) and LNCaP cells and PC-3 cells

| Comparison | Significant probes (diff. score >13) | Probes with significant difference (Δ β > 0.15) | Probes with assigned gene names | Unique genes |
|---|---|---|---|---|
| Hypermethylated in PC-3-SAM versus PC-3 | 196 | 113 | 83 | 49 |
| Hypomethylated in PC-3-SAM versus PC-3 | 116 | 103 | 80 | 34 |
| Hypermethylated in low invasive LNCaP versus PC-3 | 58 136 | 44 216 | 31 873 | 9551 |
| Hypomethylated in low invasive LNCaP versus PC-3 | 183 719 | 129 351 | 86 458 | 16 655 |

Genomic DNA was extracted, bisulfite treated and analysed on Illumina 450K bead arrays. Genome studio was used to analyse the data and identify statistically significant differences (diff score > 0.13 and Δ β >0.15).
PC-3, PC3 cells treated with 250 μM of SAM ($n$ = 3) and LNCaP cells ($n$ = 2).

liver cirrhosis and increased risk of liver cancer (Lu and Mato, 2005). Feeding rodents with a methyl donor-deficient diet indeed causes hypomethylation and activation of oncogenes resulting in liver cancer development (Zapisek *et al.*, 1992; Asada *et al.*, 2006). We have previously shown that SAM, the ubiquitous methyl donor, could lead to silencing of pro-metastatic genes in breast and prostate cancer cell lines, whereas no such effect was seen in SAH or vehicle-treated control cells (Pakneshan *et al.*, 2004; Shukeir *et al.*, 2006). In this study, we addressed the possibility that a pharmacological methyl group donor could limit skeletal metastasis, one of the most morbid aspects of prostate cancer progression. Two human prostate cancer cell lines representing late-stage human prostate cancer DU-145 and PC-3 were used in this study due to their extensive characterization and their highly tumourigenic and metastatic nature and treated with SAM concentrations previously established by us to be most effective (Shukeir *et al.*, 2006). Treatment of both cell lines resulted in a dose-dependent inhibition in their proliferative and migration rates as well as their invasive capabilities (Figure 1). Moreover, SAM treatment also resulted in diminished capabilities of both cell lines to form colonies in soft agar, an indication that their tumourigenic potential is markedly hindered following treatment (Figure 2A). Cell cycle analysis carried out indicated that the decreased proliferative and tumourigenic capabilities of both cell lines following treatment was due to an increase in the number of cells arresting in the $G_2$/M cell cycle phase (Figure 2B). Analysis of the genes that are hypermethylated in response to SAM revealed several genes that are involved in critical signalling pathways that are known to affect cell cycle.

Although both DU-145 and PC-3 cells develop skeletal lesions when injected into the tibia of SCID mice, the effect of SAM on skeletal metastasis development was further tested using the PC-3 model as it is more penetrant (up to 100% lesion development) compared with the DU-145 model. Additionally, given sufficient time, the skeletal lesions developing from PC-3 cells are of the osteolytic variety as compared with the mixed osteoblastic/osteolytic lesions observed with DU-145 allowing for a better understanding of the effect of SAM on skeletal metastasis. Pretreatment of PC-3 cells with 250 μM SAM resulted in a significant reduction in lesion size compared with animals injected with control cells (treated with 250 μM SAH). These effects could not only be explained by the growth arrest caused by SAM as overlapping or distinct pathways may be involved in tumour growth and metastasis (Steeg and Theodorescu, 2008). μCT and 3D construction revealed the extent of bone destruction observed in the control group (Figures 3 and 4). Furthermore, not only did the bones from the SAM group have a higher degree of BV/TV ratio, the bones were in a much healthier state by having smaller trabecular spacing and higher connectivity density as compared with bones extracted from control mice (Figure 4). Although our study measures the final stage of the metastasis process, namely the ability of cells to colonize the bone, our findings warrant further investigation into *in vivo* models of metastasis with *in vivo* treatments and real-time imaging.

Bone lesion development requires that cancer cells metastasize to and colonize the skeleton through homing of cancer cells to the skeleton and, once there, establishment of a viable bone colony. In this study, we demonstrate that treatment of PC-3 cells with SAM results in the reduction of several pro-metastatic genes including *uPA*, *MMP2*, *TGF-β*, *TGFBR2* and *RUNX2*, all of which play significant roles in the establishment of skeletal lesions. Reduced expression of these genes could be a direct effect of SAM treatment, or an indirect effect with SAM causing the methylation and silencing of activators/enhancers of transcription of these genes since genome-wide analysis did not reveal a change in the methylation state of these genes but rather in upstream signalling pathways (Table 2). The concern that SAM treatment might, as a global non-specific treatment modality, lead to methylation of genes in late-stage cancer such as tumour suppressor genes, which could lead to an acceleration of tumourigenesis has already been addressed by us previously where it was established that no such effects are observed (Shukeir *et al.*, 2006). To address the questions here, we performed a genome-wide DNA methylation analysis using Illumina 450K bead arrays, which give a highly representative coverage of TSS regions as well as other regulatory regions in bodies of genes as well as outside of the genes. To our surprise, the effects of SAM are highly selective and limited. SAM targets mainly genes that are aberrantly demethylated in invasive cancer (Table 1). These altered genes seem to fall into signalling pathways that are known to promote cancer growth and metastasis (Table 2). There is no evidence in our data that

## Table 2

Ingenuity pathway analysis of hypermethylated genes in SAM-treated PC3 cells

| Ingenuity canonical pathways | -log(*P*-value) | *P*-value | Ratio | Molecules |
|---|---|---|---|---|
| JAK/Stat signalling | 5.34E00 | 4.57088E-06 | 5.71E-02 | STAT5A,GNAQ,STAT3,STAT5B |
| Role of JAK family kinases in IL-6-type cytokine signalling | 5.02E00 | 9.54993E-06 | 1.11E-01 | STAT5A,STAT3,STAT5B |
| IL-9 signalling | 4.61E00 | 2.45471E-05 | 7.5E-02 | STAT5A,STAT3,STAT5B |
| Oncostatin M signalling | 4.61E00 | 2.45471E-05 | 8.57E-02 | STAT5A,STAT3,STAT5B |
| Role of JAK2 in hormone-like cytokine signalling | 4.61E00 | 2.45471E-05 | 8.33E-02 | STAT5A,STAT3,STAT5B |
| ErbB2-ErbB3 signalling | 3.93E00 | 0.00011749 | 5E-02 | STAT5A,STAT3,STAT5B |
| TREM1 signalling | 3.88E00 | 0.000131826 | 4.23E-02 | STAT5A,STAT3,STAT5B |
| IL-15 signalling | 3.84E00 | 0.000144544 | 4.48E-02 | STAT5A,STAT3,STAT5B |
| Role of JAK1 and JAK3 in γc cytokine signalling | 3.82E00 | 0.000151356 | 4.48E-02 | STAT5A,STAT3,STAT5B |
| Growth hormone signalling | 3.68E00 | 0.00020893 | 3.95E-02 | STAT5A,STAT3,STAT5B |
| IL-3 signalling | 3.64E00 | 0.000229087 | 4.05E-02 | STAT5A,STAT3,STAT5B |
| Prolactin signalling | 3.61E00 | 0.000245471 | 3.75E-02 | STAT5A,STAT3,STAT5B |
| Acute myeloid leukaemia signalling | 3.54E00 | 0.000288403 | 3.66E-02 | STAT5A,STAT3,STAT5B |
| Role of tissue factor in cancer | 3.1E00 | 0.000794328 | 2.63E-02 | STAT5A,GNAQ,STAT5B |
| Regulation of eIF4 and p70S6K signalling | 2.71E00 | 0.001949845 | 1.71E-02 | EIF1AY,RPS4Y1,RPS4Y2 |
| IL-2 signalling | 2.45E00 | 0.003548134 | 3.45E-02 | STAT5A,STAT5B |
| Oestrogen-dependent breast cancer signalling | 2.31E00 | 0.004897788 | 2.78E-02 | STAT5A,STAT5B |
| Glucocorticoid receptor signalling | 2.03E00 | 0.009332543 | 1.02E-02 | STAT5A,STAT3,STAT5B |
| Chronic myeloid leukaemia signalling | 1.96E00 | 0.010964782 | 1.9E-02 | STAT5A,STAT5B |
| PPAR signalling | 1.96E00 | 0.010964782 | 1.9E-02 | STAT5A,STAT5B |
| Androgen signalling | 1.82E00 | 0.015135612 | 1.4E-02 | GNAQ,SRY |
| PPARα/RXRα activation | 1.49E00 | 0.032359366 | 1.09E-02 | GNAQ,STAT5B |
| Ephrin receptor signalling | 1.47E00 | 0.033884416 | 1E-02 | GNAQ,STAT3 |
| EIF2 signalling | 1.41E00 | 0.038904514 | 9.9E-03 | RPS4Y1,RPS4Y2 |
| Role of JAK1, JAK2 and TYK2 in interferon signalling | 1.4E00 | 0.039810717 | 3.7E-02 | STAT3 |
| mTOR signalling | 1.39E00 | 0.040738028 | 9.48E-03 | RPS4Y1,RPS4Y2 |
| EGF signalling | 1.13E00 | 0.074131024 | 1.92E-02 | STAT3 |
| Endometrial cancer signalling | 1.07E00 | 0.085113804 | 1.75E-02 | CTNNA1 |
| ERK5 signalling | 9.95E-01 | 0.101157945 | 1.54E-02 | GNAQ |
| Chemokine signalling | 9.57E-01 | 0.110407862 | 1.37E-02 | GNAQ |
| Molecular mechanisms of cancer | 9.55E-01 | 0.110917482 | 5.31E-03 | CTNNA1,GNAQ |
| Ephrin B signalling | 9.34E-01 | 0.116412603 | 1.25E-02 | GNAQ |
| PDGF signalling | 9.12E-01 | 0.12246162 | 1.18E-02 | STAT3 |
| Cytotoxic T lymphocyte-mediated apoptosis of target cells | 8.97E-01 | 0.126765187 | 1.18E-02 | HLA-DRB5 |
| Allograft rejection signalling | 8.87E-01 | 0.129717927 | 1.05E-02 | HLA-DRB5 |
| OX40 signalling pathway | 8.72E-01 | 0.134276496 | 1.06E-02 | HLA-DRB5 |
| FGF signalling | 8.67E-01 | 0.135831345 | 1.09E-02 | STAT3 |
| VEGF signalling | 8.63E-01 | 0.137088177 | 1.01E-02 | EIF1AY |
| IGF-1 signalling | 8.19E-01 | 0.151705037 | 9.52E-03 | STAT3 |
| HGF signalling | 8.11E-01 | 0.154525444 | 9.52E-03 | STAT3 |
| Pancreatic adenocarcinoma signalling | 7.8E-01 | 0.165958691 | 8.33E-03 | STAT3 |
| Role of NANOG in mammalian embryonic stem cell pluripotency | 7.72E-01 | 0.169044093 | 8.77E-03 | STAT3 |
| GNRH signalling | 7.18E-01 | 0.191425593 | 6.8E-03 | GNAQ |
| Relaxin signalling | 6.91E-01 | 0.203704208 | 6.33E-03 | GNAQ |
| CXCR4 signalling | 6.45E-01 | 0.226464431 | 5.99E-03 | GNAQ |
| Tight junction signalling | 6.4E-01 | 0.229086765 | 6.21E-03 | CTNNA1 |
| Gap junction signalling | 6.35E-01 | 0.231739465 | 5.68E-03 | GNAQ |
| Cdc42 signalling | 6.23E-01 | 0.238231947 | 5.65E-03 | HLA-DRB5 |
| Wnt/β-catenin signalling | 6.02E-01 | 0.250034536 | 5.78E-03 | GNAQ |
| RhoGDI signalling | 5.96E-01 | 0.253512863 | 5.08E-03 | GNAQ |
| ILK signalling | 5.69E-01 | 0.269773943 | 5.21E-03 | TMSB4Y |
| ERK/MAPK signalling | 5.67E-01 | 0.271019163 | 4.85E-03 | STAT3 |
| Leukocyte extravasation signalling | 5.63E-01 | 0.273526873 | 5.08E-03 | CTNNA1 |
| Breast cancer regulation by Stathmin1 | 5.57E-01 | 0.27733201 | 4.83E-03 | GNAQ |
| Actin cytoskeleton signalling | 5.17E-01 | 0.304088503 | 4.2E-03 | TMSB4Y |
| Signalling by Rho family GTPases | 4.91E-01 | 0.322849412 | 3.97E-03 | GNAQ |
| PLC signalling | 4.88E-01 | 0.325087297 | 3.85E-03 | GNAQ |
| Colorectal cancer metastasis signalling | 4.77E-01 | 0.333426413 | 3.89E-03 | STAT3 |

SAM targets tumour suppressor genes. These data lend support to the use of SAM to control bone metastasis.

Our results indicate that SAM treatment might be a useful therapy for late-stage prostate cancer, which has a high potential to develop skeletal metastasis. The DU-145 and PC-3 prostate cancer cell lines exhibit high levels of glycine N-methyltransferase (GNMT), an enzyme that catalyses the breakdown of SAM into its inactive form SAH (Song *et al.*, 2011). The high expression of GNMT, coupled with the unstable nature of SAM could explain the relatively high concentrations needed to achieve an effective response. Nevertheless, the effective SAM concentrations used in this study are in line with therapeutic doses utilized in other malignancies and tumour models (Lu *et al.*, 2009; Tomasi *et al.*, 2012). We would like to propose a model whereby SAM treatment targets tumour cells and limits their tumourigenic and metastatic potential by hypermethylating and silencing genes and gene pathways involved in cell cycle control and metastasis, arresting the cells in the $G_2$/M phase of the cell cycle. Those tumour cells, which escape the inhibitory effects would have decreased levels of pro-metastatic gene pathways such as those triggered by *uPA* and *MMP2*, which we have previously shown to be silenced by hypermethylation in PC-3 cells in response to SAM (Shukeir *et al.*, 2006). In addition, our genome-wide analysis revealed the JAK/STAT pathway as a main pathway triggered by methylation with SAM (Table 2). Several STAT genes are hypermethylated by SAM including *STAT3* (Figure 5 for gene expression silencing by SAM), *STAT5A* and *STAT5B* (Supporting Information Table S1). These genes are involved in several pathways that are known to be involved in metastasis such as the EFG, WNT/β-catenin, RHO and tight junction signalling and other signalling pathways highlighted in Table 2. We demonstrated that a STAT3 inhibitor leads to inhibition of PC-3 cell invasiveness (Figure 5). In addition, we demonstrate that genes, which play important roles in homing tumour cells invasion and metastasis such as uPA, and genes, which are critical in establishment and maintaining of skeletal lesions such as *TGF-β*, *TGFBR2* and *RUNX2*, are silenced by SAM.

Taken together, these data elucidate the potential use of SAM as a pharmacological agent to limit skeletal metastasis in prostate cancer. The remarkable selectivity of SAM revealed here is surprising and alleviates concerns that it would target a large fraction of the genome. None of the genes that are methylated are tumour suppressor genes; thus, our data support the idea that SAM treatment could alleviate the burden of bone metastasis without stimulating further tumour growth. Of additional interest is that SAM is an approved nutritional supplement whose daily intake has been shown to provide beneficial effects against many ailments such as depression, liver disease and potentially Alzheimer's disease (Lee *et al.*, 2012; Papakostas *et al.*, 2012; Mato *et al.*, 2013). In addition, our data suggest a possible chemo-preventive role for SAM against prostate tumour development and open the door to studies on chronic effects of low dietary SAM doses in cancer prevention.

## Acknowledgements

This work was supported by a grant MOP 130410 from the Canadian Institutes for Health Research to S. A. R. and M. S.

## Author contributions

N. S. and A. A. established all doses and conditions for various *in vitro* and *in vivo* studies and generated the data presented. N. S. also wrote the manuscript with S. A. R. and M. S.

B. S. and F. C. performed genome-wide methylation analyses, designed methylation primers and analysed the results with NS.

S. P. carried out methylation analysis studies related to STAT3.

A. A. carried out various *in vitro* and *in vivo* studies and analysed the resulted with N. S.

S. A. R. and M. S. designed the entire study, supervised various aspects of the project, wrote and corrected the manuscript.

## Conflict of interest

None.

## References

Alexander SPH, Benson HE, Faccenda E, Pawson AJ, Sharman JL, Spedding M *et al.* (2013a). The Concise Guide to PHARMACOLOGY 2013/14: G protein-coupled receptors. Br J Pharmacol 170: 1459–1581.

Alexander SPH, Benson HE, Faccenda E, Pawson AJ, Sharman JL, Spedding M *et al.* (2013b). The Concise Guide to PHARMACOLOGY 2013/14: Nuclear hormone receptors. Br J Pharmacol 170: 1652–1675.

Alexander SPH, Benson HE, Faccenda E, Pawson AJ, Sharman JL, Spedding M *et al.* (2013c). The Concise Guide to PHARMACOLOGY 2013/14: Catalytic receptors. Br J Pharmacol 170: 1676–1705.

Alexander SPH, Benson HE, Faccenda E, Pawson AJ, Sharman JL, Spedding M *et al.* (2013d). The Concise Guide to PHARMACOLOGY 2013/14: Enzymes. Br J Pharmacol 170: 1797–1867.

Anstee QM, Day CP (2012). S-adenosylmethionine (SAMe) therapy in liver disease: a review of current evidence and clinical utility. J Hepatol 57: 1097–1109.

Asada K, Kotake Y, Asada R, Saunders D, Broyles RH, Towner RA *et al.* (2006). LINE-1 hypomethylation in a choline-deficiency-induced liver cancer in rats: dependence on feeding period. J Biomed Biotechnol 2006: 17142.

Ateeq B, Unterberger A, Szyf M, Rabbani SA (2008). Pharmacological inhibition of DNA methylation induces proinvasive and prometastatic genes in vitro and in vivo. Neoplasia 10: 266–278.

Bussard KM, Gay CV, Mastro AM (2008). The bone microenvironment in metastasis; what is special about bone? Cancer Metastasis Rev 27: 41–55.

Chen G, Shukeir N, Potti A, Sircar K, Aprikian A, Goltzman D *et al.* (2004). Up-regulation of Wnt-1 and beta-catenin production in patients with advanced metastatic prostate carcinoma: potential pathogenetic and prognostic implications. Cancer 101: 1345–1356.

Chen G, Sircar K, Aprikian A, Potti A, Goltzman D, Rabbani SA (2006). Expression of RANKL/RANK/OPG in primary and metastatic human prostate cancer as markers of disease stage and functional regulation. Cancer 107: 289–298.

Chik F, Machnes Z, Szyf M (2014). Synergistic anti-breast cancer effect of a combined treatment with the methyl donor S-adenosyl methionine and the DNA methylation inhibitor 5-aza-2′-deoxycytidine. Carcinogenesis 35: 138–144.

Detich N, Hamm S, Just G, Knox JD, Szyf M (2003). The methyl donor S-adenosylmethionine inhibits active demethylation of DNA: a candidate novel mechanism for the pharmacological effects of S-adenosylmethionine. J Biol Chem 278: 20812–20820.

Devarajan E, Huang S (2009). STAT3 as a central regulator of tumor metastases. Curr Mol Med 9: 626–633.

Fernandez AF, Assenov Y, Martin-Subero JI, Balint B, Siebert R, Taniguchi H *et al.* (2012). A DNA methylation fingerprint of 1628 human samples. Genome Res 22: 407–419.

Gu L, Dagvadorj A, Lutz J, Leiby B, Bonuccelli G, Lisanti MP *et al.* (2010). Transcription factor Stat3 stimulates metastatic behavior of human prostate cancer cells in vivo, whereas Stat5b has a preferential role in the promotion of prostate cancer cell viability and tumor growth. Am J Pathol 176: 1959–1972.

Gupta GP, Massague J (2006). Cancer metastasis: building a framework. Cell 127: 679–695.

Heath VL, Bicknell R (2009). Anticancer strategies involving the vasculature. Nat Rev Clin Oncol 6: 395–404.

Hoffmann MJ, Schulz WA (2005). Causes and consequences of DNA hypomethylation in human cancer. Biochem Cell Biol 83: 296–321.

Jiang Y, Dai J, Zhang H, Sottnik JL, Keller JM, Escott KJ *et al.* (2013). Activation of the Wnt pathway through use of AR79, a glycogen synthase kinase 3beta inhibitor, promotes prostate cancer growth in soft tissue and bone. Mol Cancer Res 11: 1597–1610.

Juarez P, Guise TA (2011). TGF-beta in cancer and bone: implications for treatment of bone metastases. Bone 48: 23–29.

Kessenbrock K, Plaks V, Werb Z (2010). Matrix metalloproteinases: regulators of the tumor microenvironment. Cell 141: 52–67.

Kilkenny C, Browne W, Cuthill IC, Emerson M, Altman DG (2010). Animal research: Reporting *in vivo* experiments: the ARRIVE guidelines. Br J Pharmacol 160: 1577–1579.

Kwaan HC, McMahon B (2009). The role of plasminogen-plasmin system in cancer. Cancer Treat Res 148: 43–66.

Lee S, Lemere CA, Frost JL, Shea TB (2012). Dietary supplementation with S-adenosyl methionine delayed amyloid-beta and tau pathology in 3xTg-AD mice. J Alzheimers Dis 28: 423–431.

Lu SC, Mato JM (2005). Role of methionine adenosyltransferase and S-adenosylmethionine in alcohol-associated liver cancer. Alcohol 35: 227–234.

Lu SC, Ramani K, Ou X, Lin M, Yu V, Ko K *et al.* (2009). S-adenosylmethionine in the chemoprevention and treatment of hepatocellular carcinoma in a rat model. Hepatology 50: 462–471.

Mato JM, Martinez-Chantar ML, Lu SC (2013). S-adenosylmethionine metabolism and liver disease. Ann Hepatol 12: 183–189.

McGrath J, Drummond G, McLachlan E, Kilkenny C, Wainwright C (2010). Guidelines for reporting experiments involving animals: the ARRIVE guidelines. Br J Pharmacol 160: 1573–1576.

Mishra DK, Chen Z, Wu Y, Sarkissyan M, Koeffler HP, Vadgama JV (2010). Global methylation pattern of genes in androgen-sensitive and androgen-independent prostate cancer cells. Mol Cancer Ther 9: 33–45.

Pakneshan P, Szyf M, Farias-Eisner R, Rabbani SA (2004). Reversal of the hypomethylation status of urokinase (uPA) promoter blocks breast cancer growth and metastasis. J Biol Chem 279: 31735–31744.

Papakostas GI, Cassiello CF, Iovieno N (2012). Folates and S-adenosylmethionine for major depressive disorder. Can J Psychiatry 57: 406–413.

Pawson AJ, Sharman JL, Benson HE, Faccenda E, Alexander SP, Buneman OP *et al.*; NC-IUPHAR (2014). The IUPHAR/BPS Guide to PHARMACOLOGY: an expert-driven knowledgebase of drug targets and their ligands. Nucl Acids Res 42 (Database Issue): D1098–D106.

Richiardi L, Fiano V, Grasso C, Zugna D, Delsedime L, Gillio-Tos A *et al.* (2013). Methylation of APC and GSTP1 in non-neoplastic tissue adjacent to prostate tumour and mortality from prostate cancer. PLoS ONE 8: e68162.

Shukeir N, Pakneshan P, Chen G, Szyf M, Rabbani SA (2006). Alteration of the methylation status of tumor-promoting genes decreases prostate cancer cell invasiveness and tumorigenesis in vitro and in vivo. Cancer Res 66: 9202–9210.

Siegel R, Naishadham D, Jemal A (2013). Cancer statistics, 2013. CA Cancer J Clin 63: 11–30.

Song YH, Shiota M, Kuroiwa K, Naito S, Oda Y (2011). The important role of glycine N-methyltransferase in the carcinogenesis and progression of prostate cancer. Mod Pathol 24: 1272–1280.

Steeg PS (2006). Tumor metastasis: mechanistic insights and clinical challenges. Nat Med 12: 895–904.

Steeg PS, Theodorescu D (2008). Metastasis: a therapeutic target for cancer. Nat Clin Pract Oncol 5: 206–219.

Stefanska B, Huang J, Bhattacharyya B, Suderman M, Hallett M, Han ZG *et al.* (2011). Definition of the landscape of promoter DNA hypomethylation in liver cancer. Cancer Res 71: 5891–5903.

Stefanska B, Cheishvili D, Suderman M, Arakelian A, Huang J, Hallett M *et al.* (2014). Genome-wide study of hypomethylated and induced genes in patients with liver cancer unravels novel anticancer targets. Clin Cancer Res 20: 3118–3132.

Sturge J, Caley MP, Waxman J (2011). Bone metastasis in prostate cancer: emerging therapeutic strategies. Nat Rev Clin Oncol 8: 357–368.

Sun X, Cheng G, Hao M, Zheng J, Zhou X, Zhang J *et al.* (2010). CXCL12/CXCR4/CXCR7 chemokine axis and cancer progression. Cancer Metastasis Rev 29: 709–722.

Suva LJ, Washam C, Nicholas RW, Griffin RJ (2011). Bone metastasis: mechanisms and therapeutic opportunities. Nat Rev Endocrinol 7: 208–218.

Tomasi ML, Tomasi I, Ramani K, Pascale RM, Xu J, Giordano P *et al.* (2012). S-adenosyl methionine regulates ubiquitin-conjugating enzyme 9 protein expression and sumoylation in murine liver and human cancers. Hepatology 56: 982–993.

Zapisek WF, Cronin GM, Lyn-Cook BD, Poirier LA (1992). The onset of oncogene hypomethylation in the livers of rats fed methyl-deficient, amino acid-defined diets. Carcinogenesis 13: 1869–1872.

## Supporting information

Additional Supporting Information may be found in the online version of this article at the publisher's web-site:

http://dx.doi.org/10.1111/bph.13102

**Figure S1** Effect of SAM treatment on expression of tumor suppressor genes.